Materials and Design 160 (2018) 572–577

Contents lists available at ScienceDirect

Materials and Design

journal homepage: www.elsevier.com/locate/matdes

# Ag nanowire electrode with patterned dry film photoresist insulator for flexible organic light-emitting diode with various designs

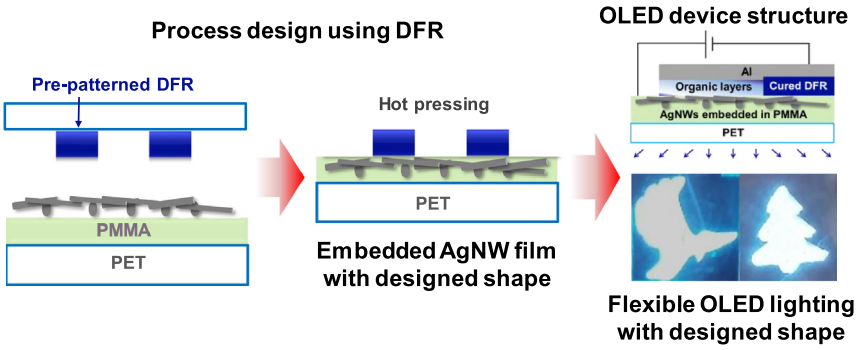
Sunho Kim [a,b], Byungil Hwang [c,*]

[a] School of Advanced Materials Science and Engineering, Sungkyunkwan University, Suwon, Republic of Korea
[b] Post-Silicon Semiconductor Institute, Korea Institute of Science and Technology, Seoul 02792, Republic of Korea
[c] School of Integrative Engineering, Chung-Ang University, Seoul 06974, Republic of Korea

## HIGHLIGHTS

- Ag nanowire flexible transparent electrodes with root mean square below 5 nm were fabricated by a single hot pressing process
- By using pre-patterned dry film photoresist, shaped Ag nanowire electrodes were fabricated in the same hot pressing process
- Flexible organic light-emitting diode lightings with various designs were realized with the fabricated electrodes
- Paper-based organic light-emitting diode lighting was realized using a dry film photoresist planarization layer

## GRAPHICAL ABSTRACT




## ARTICLE INFO

*Article history:*
Received 18 April 2018
Received in revised form 27 September 2018
Accepted 28 September 2018
Available online 2 October 2018

*Keywords:*
Dry film photoresist
Silver nanowire
Insulator
Electrode
Paper
Organic light-emitting diode

## ABSTRACT

In this study, the utilization of a dry film photoresist (DFR) was explored for fabricating a patterned insulating layer in Ag nanowire (AgNW) bottom electrodes with various designs for flexible organic light-emitting diodes (OLEDs). With a single hot-pressing step, a pre-patterned DFR insulator was attached onto the AgNW electrodes, thus forming insulated electrodes in desired patterns. In the same hot-pressing step, AgNWs were also embedded into poly(methyl methacrylate), which sufficiently reduced the root mean square (RMS) roughness (~5 nm) for use in OLED lighting. Using DFR, AgNW electrodes with various shapes were fabricated to realize shaped flexible OLED lighting. The performance of OLED lighting employing the AgNW/patterned-DFR insulator electrode was comparable to that of indium-tin-oxide-based OLED lighting. Further, the DFR insulator was utilized as a planarization layer in a paper-based OLED lighting, which operated well with a turn-on voltage of 3.5 V and maximum luminance of 157 cd/m$^2$ at 7.5 V.

© 2018 Elsevier Ltd. This is an open access article under the CC BY-NC-ND license (http://creativecommons.org/licenses/by-nc-nd/4.0/).

## 1. Introduction

With increasing interest in flexible organic light-emitting diode (OLED) lightings, the development of flexible transparent electrodes has become crucial for securing the reliability of devices under harsh mechanical strains [1–6]. Indium tin oxide (ITO) is commonly used for the electrodes of OLEDs; however, its intrinsic brittleness and high processing temperature limit its use in flexible OLEDs built on polymer substrates [7,8]. As alternatives of ITO, various material systems such as metal grids [9,10], carbon nanotubes [11,12], graphene [13,14], and metal nanowires [15–20] have been reported. Among these, Ag nanowires (AgNWs) are the most promising alternative owing to their high conductivity and transparency, which are comparable to those of ITO

* Corresponding author.
*E-mail address:* bihwang@cau.ac.kr (B. Hwang).

https://doi.org/10.1016/j.matdes.2018.09.051
0264-1275/© 2018 Elsevier Ltd. This is an open access article under the CC BY-NC-ND license (http://creativecommons.org/licenses/by-nc-nd/4.0/).

[21,22]. In addition, AgNWs have attracted the attention of electronics industry owing to their potential for scalable synthesis and ease of formation of large-scale conductive films on polymer substrates via simple coating methods such as bar coating, slot-die coating, and spray coating [23–26].

However, for OLED applications, the roughness of AgNW networks should be lower than ~10 nm. Stacked one-dimensional AgNWs on a substrate typically have a high surface roughness of more than a few hundred nanometers, where concentrated current causes the degradation of OLED performance; consequently, a dark spot appears on the OLED lighting panels. Typically, a reduction in the roughness of AgNW electrodes is achieved by embedding AgNWs into the surface of polymeric resins [27]. In the embedding process, AgNWs are first coated on a substrate, and then, a UV or thermally curable resin is deposited on the AgNWs and cured. During curing, AgNWs are bound to the surface of the resins. By detaching the cured resin from the substrate, a AgNW electrode embedded in the resin is fabricated. In addition, the embedding process can remarkably reduce the roughness of the AgNW to ~5 nm [27,28], which is sufficient for OLED lighting. However, the use of embedding process in the industry is limited owing to its complexity, as it includes curing and detachment steps, and the potential loss of conductivity during the detachment process. Moreover, an additional step to coat the insulating layer is required to obtain shaped or designed OLED lighting panels [29]. The typical liquid-type resin used for the insulating layer not only increases the complexity of the fabrication process with additional coating and curing steps, but also hinders its use in electrodes on a paper-based substrate. The increased number of fabrication steps as well as the limited application area due to the complexity of the aforementioned embedding process and the liquid resin-based insulating process increases the processing and material costs, thereby limiting the use of AgNWs in the flexible OLED lighting industry. Therefore, a new process design for the simple fabrication of flexible and transparent AgNW electrodes with low roughness below ~10 nm and good compatibility with various substrates, including paper-based substrates, should be developed to widen the application areas of AgNW electrodes in the flexible OLED lighting industry.

In the present study, a simple and cost-effective fabrication process to prepare AgNW electrodes with low roughness for flexible and patterned OLED lighting is designed using a simple hot pressing technique with a dry film photoresist (DFR) insulating layer. DFR is a solid-film-type negative photoresist that can be attached on any type of substrate, such as polymer, glass, paper, and ceramic, by simple lamination or hot pressing. Herein, AgNW electrodes with designed patterns were fabricated by using a pre-patterned DFR, and the roughness of the AgNWs was remarkably reduced by embedding the AgNWs into poly(methyl methacrylate) (PMMA) having a low melting temperature ($T_m$). AgNW electrodes embedded in PMMA with the designed patterns of an insulating layer were easily fabricated using a single hot-pressing step without requiring complex coating and detachment processes or any additional step to form the insulating layer. The shaped OLED lighting employing the AgNW/patterned-DFR insulator electrode demonstrates good performance, comparable to that of ITO-based OLED lighting. Furthermore, the utilization of DFR insulator for OLED lighting has also been demonstrated for paper-based OLED lighting.

## 2. Experiment

### 2.1. Materials

PMMA powder (Aldrich, M.W.: 996,000) was dissolved in water with anisole ($CH_3OC_6H_5$, Daejung) to prepare a 4 wt% PMMA solution. AgNW suspension in isopropyl alcohol with 1 wt% solid content was purchased from Nanopixis Co. Ltd., and the average diameter and length of the AgNWs were ~35 nm and ~25 μm, respectively. Roll-type DFR films (KL-1015) with 50-mm length, 15-mm thickness, and 30-mm width were purchased from KOLON Industries. Hot press equipment was used to embed the AgNWs into PMMA.

To fabricate the AgNWs/PMMA/PET electrodes, a Mayer rod (#6, RD Specialist Inc.) was used to coat PMMA on the poly(ethylene terephthalate) (PET) substrate, and then, AgNWs were coated on the PMMA/PET substrate. Meanwhile, the DFR/cover film was UV-cured with a patterned photomask. Afterward, a $Na_2CO_3$ aqueous solution (1 wt%) was used to develop the un-cured region of DFR. The DFR/cover film and the AgNWs/PMMA/PET film were then hot-pressed at 150 °C under 40 MPa for 5 min.

For the paper-based electrode, a silver nanoparticle (AgNP) suspension in ethanol with 50 wt% solid content was purchased from N&B, and the average diameter of the AgNPs was ~50 nm. A super-hydrophobic PET (SHP-PET) film (SKC, thickness: 25 μm), paper (milk, A4 80 g), black toner (HP, CF210A), and office laser printer (HP, M276nw) were used in the dry transfer process.

To prepare the paper-based electrodes, the dry transfer method using toner-printed paper was used. First, AgNPs were coated on the SHP-PET film. Then, the AgNPs on SHP-PET were placed on the toner-printed paper and hot-pressed to transfer and embed them in the toner. The DFR prepared using the same method as that used to prepare the AgNPs/PMMA/PET film was subsequently placed and hot-pressed on the AgNPs/toner/paper electrodes, thereby forming a patterned insulating layer. The detailed mechanism of the transfer process using the toner-printed paper is reported elsewhere [30].

### 2.2. OLED fabrication

To fabricate a bottom-emitting blue OLED, the following layers were thermally evaporated on the DFR/AgNWs/PMMA/PET film and ITO glass: 1,4,5,8,9,11-Hexaazatriphenylene-hexacarbonitrile, 60 nm/DS-HTL, 40 nm/2-methyl-9,10-di(2-naphthyl) anthracene: 5 wt% 1,6-bis (*N*-phenyl-p-CN-phenylamino)-pyrenes, 20 nm/LG-201:Liq (1:1), 30 nm/Liq, 1.5 nm/Al, 100 nm. To fabricate a paper-based top-emitting blue OLED, 10-nm-thick Al layer and 10-nm-thick Ag layer were deposited using a shadow mask; these layers functioned as semi-transparent top electrodes. Organic layers and a cathode metal layer were deposited under $8 \times 10^{-7}$ Torr in a vacuum evaporator with deposition rates of 0.1 and 1 Å/s, respectively. The current–

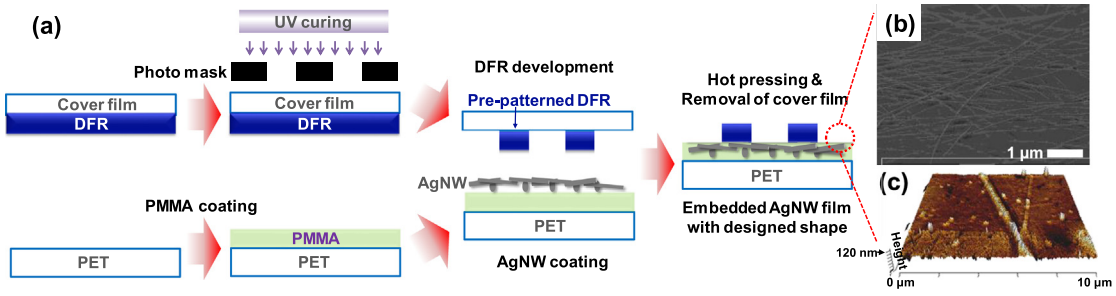



**Fig. 1.** (a) Schematic illustrations of fabrication step of patterned and embedded AgNW electrodes with DFR insulating layer. (b) 35° tilted SEM image and (c) AFM image of AgNWs embedded into PMMA.

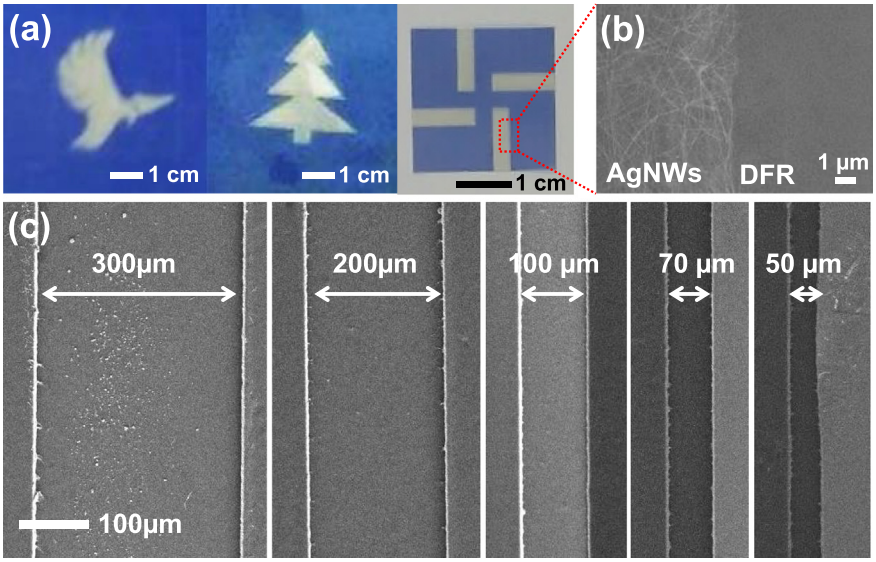



**Fig. 2.** (a) Photographs of pre-patterned DFR with various shapes attached on the AgNW/PMMA/PET electrodes. (b) SEM images obtained at the edge between AgNWs and DFR, and (c) pre-patterned DFR with different line widths.

voltage–luminance characteristics were measured using a Keithley 236 source measurement unit and a Minolta CS2000 spectroradiometer (Fig. S1).

## 3. Results and discussion

A schematic illustration of the fabrication process of the AgNW electrodes embedded into PMMA with the DFR insulator is presented in Fig. 1(a). To successfully embed the AgNWs into the polymeric films, the $T_m$ of the polymer films should be sufficiently low to allow the polymer to be melted partially during the hot pressing process. As typical AgNWs agglomerate over ~180 °C [31,32], the appropriate $T_m$ of the polymeric films should be lower than ~180 °C. Therefore, the first step in the fabrication of AgNW electrodes with desirable designs was the coating of PMMA onto the PET film. PMMA with a $T_m$ of ~160 °C was considered an appropriate intermediate polymer into which the AgNWs were embedded by hot pressing, whereas PET with excellent optical and mechanical properties exhibited a good performance as the base substrate for OLED lighting. Subsequently, the DFR with a cover film was UV-cured using a photomask in the desired patterns. After curing, the un-cured region of the DFR was dissolved with a $Na_2CO_3$ aqueous solution (1 wt%), and the developed DFR/cover film was rinsed with deionized water. During the curing and development processes, the PET-based cover film was not damaged; thus, pre-

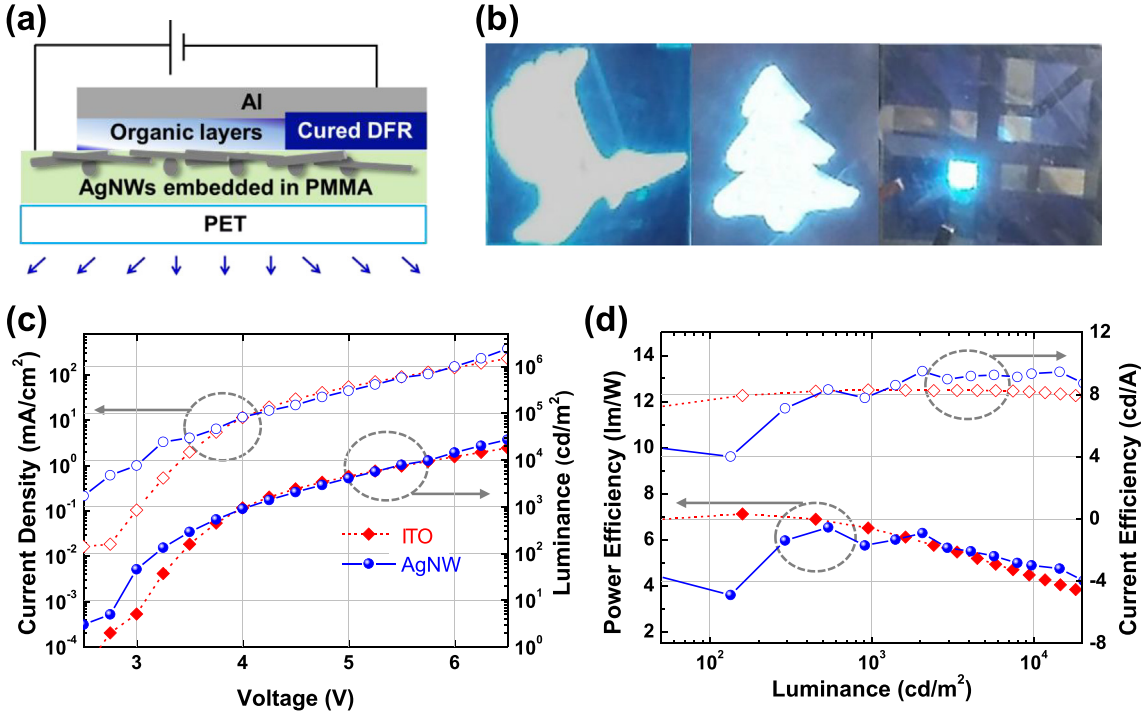



**Fig. 3.** (a) Schematic structure of OLED lighting with DFR insulator. (b) Photographs of OLED lighting with AgNW/DFR electrodes of different shapes. Electroluminescence performances of AgNW/DFR-based and ITO-based OLED lightings: (c) current density and luminance, and (d) power efficiency and current efficiency.

**Table 1**
Turn-on voltages of OLED devices employing different types of electrodes.

| Electrode type | Turn-on voltage (V) | Reference |
|---|---|---|
| ITO/glass | 3.0 | This work |
| AgNWs/PMMA/PET | 2.8 | This work |
| AgNPs/paper | 3.5 | This work |
| AgNWs/cPI | 4.5 | [1] |
| Graphene/glass | 4.2 | [13] |
| AgNWs/PET | 3.0 | [29] |

patterned DFR on a PET-based cover film could be formed, which allowed the fabrication of patterned/shaped AgNW electrodes in a single step. Subsequently, the DFR was placed on the AgNWs/PMMA/PET film and hot-pressed at 150 °C under 40 MPa for 5 min. After hot pressing, the cover film of the DFR was removed; thus, only the DFR acting as an insulator remained on the AgNWs/PMMA/PET electrodes. As mentioned above, the AgNWs were embedded into the PMMA layer during hot pressing, which reduced the roughness of AgNW electrodes. This was also confirmed by the 35° tilted SEM image taken from the surface of the AgNWs/PMMA/PET samples, as shown in Fig. 1(b). Furthermore, the RMS roughness of the AgNWs embedded into PMMA was ~4.1 nm (Fig. 1(c)), which is sufficient for OLED lighting.

The photographs of the patterned DFR/AgNWs/PMMA/PET film for a bottom electrode of OLED are shown in Fig. 2(a). The area covered by the DFR insulator is denoted in blue, whereas the transparent region shows the insulated AgNW electrode in the designed shape. To prepare flexible OLED lighting panels with various shapes, AgNW electrodes with different shapes, such as bird and tree, were fabricated using various shapes of the photomask. To compare the OLED performance of the AgNW/patterned-DRF insulator electrodes with that of the ITO electrodes, square patterns having the same dimensions as those of the commercially available ITO patterns on glass (3 mm × 11 mm) were fabricated (Fig. 2(a)). Fig. 2(a)–(b) shows that the DFR was clearly patterned during the photo-patterning process and was successfully transferred onto the AgNW electrodes, thereby yielding AgNW electrodes in the designed shapes of the DFR insulator. The microstructural SEM image of the patterned electrodes comprising the DFR insulator (Fig. 2(c)) further confirmed that the transferred DFR insulator covered the non-desirable area of the AgNWs without observable defects such as pinholes, which can expose the AgNWs and cause shorting during OLED operation. Furthermore, a sharp edge was observed between the AgNW and patterned DFR insulator, as shown in Fig. 2(c), which enabled illumination of the flexible OLED lighting system only through the designed shape.

To investigate the minimum line width to be formed by the patterned DFR insulator, AgNW electrodes with different line widths were fabricated using the photomask with line widths varying from 10 μm to 300 μm. As mentioned above, the pre-patterned DFR was fabricated by selectively curing the DFR films under UV illumination through the photomask. The region under the transparent area of the photomask was cured with UV light and became intact, whereas the uncured area was removed during the development process. However, as the pattern size decreased, a shadowing effect occurred; thus, UV light could reach even the area under the black area of the photomask designed for blocking UV light. Therefore, non-desirable curing occurred in the DFR even under the black area, which hindered the development of the DFR. In our processing system, widths up to 50 μm were patterned without any significant shadowing effect, as shown in the SEM images in Fig. 2(c). However, for pattern widths less than 30 μm, pre-patterning of DFR was difficult, which is attributed to the shadowing effect. The shadowing effect might be reduced by using a professional mask alignment system; however, the width of 50 μm is sufficiently low for fabricating shaped OLED lighting panels.

Flexible OLED lightings were fabricated using the DFR/AgNWs/PMMA/PET film with various patterns as the flexible bottom electrodes, and the schematic structure of the OLED lighting is shown in Fig. 3(a). Similar to the structure of previously reported light-emitting devices [33–35], our OLED lighting devices consisted of top and bottom electrodes and organic light-emitting layers. An Al top electrode was deposited onto the organic layers and the DFR insulating layer, which efficiently prevented contact between the AgNW bottom electrode and the Al top electrode. Therefore, OLED lightings with different patterns were successfully operated without the shorting problem, as shown in Fig. 3(b). To analyze the performance of an OLED that uses the DFR/AgNWs/PMMA/PET film, the current density — voltage–luminescence (J–V–L) and efficiency characteristics of the AgNW-based and ITO/glass-based OLED lightings were measured. Both the electrodes were patterned as 3 mm × 3 mm squares; the materials used for both the OLED lightings were the same, except for the bottom electrodes. The turn-on voltages of AgNW-based and ITO-based OLEDs were similar at 2.8 V and 3.0 V, respectively. These turn-on voltages were similar to or lower than those of the previously reported OLED devices with different types of electrodes, as summarized in Table 1. The current density of the AgNW-based OLED was higher than that of the ITO-based OLED near the turn-on voltage region (2.5–4.0 V); however, both the OLED devices exhibited similar current densities and luminances as the operating voltage increased beyond 4.0 V (Fig. 3(c)). The maximum luminances of the AgNW-based and ITO-based OLED devices were 27,341 cd/m$^2$ at 6.5 V and 22,554 cd/m$^2$ at 6.7 V, respectively. In terms of efficiency, the AgNW-based and ITO-based OLED lightings showed contrasting behaviors in the low- and high-luminance regions, as shown in Fig. 3(d). In the low-luminance region below $10^3$ cd/m$^2$, the AgNW-based OLED lighting showed lower power and current efficiencies than those of the ITO-based OLED lighting, whereas the efficiency of the former was similar to or higher than that of the latter in the high-luminance region over $10^3$ cd/m$^2$. A similar phenomenon was observed in the previous studies on AgNW-based OLED lighting [36]. In the AgNW-based OLED lighting, the planarization of AgNWs could be incomplete, which may create a leakage path, resulting in high current density in the low-luminance region; thus, the efficiency could be low

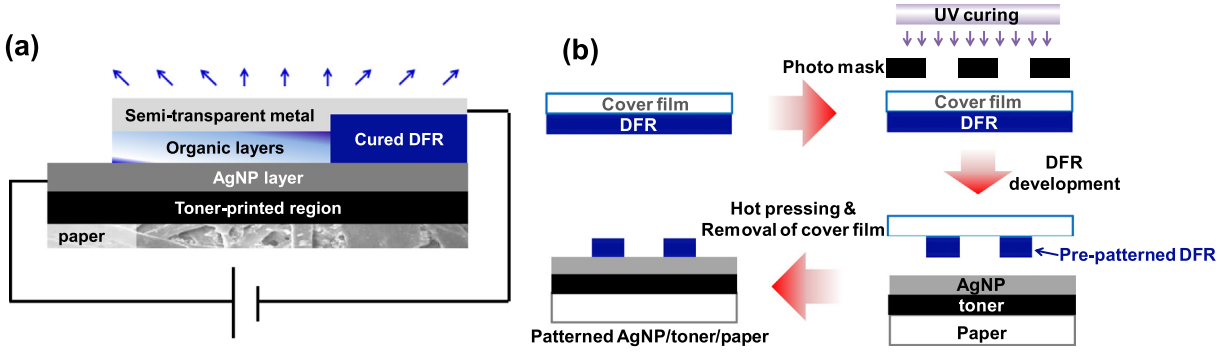



**Fig. 4.** (a) Schematic of the structure of DFR/paper-based OLED lighting, and (b) fabrication step of paper-based OLED lighting.

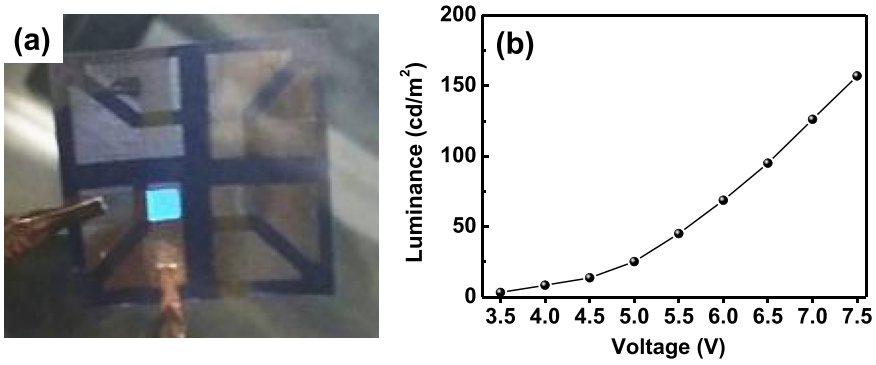



**Fig. 5.** (a) Photograph of the operation of paper-based OLED lighting, and luminance of paper-based OLED lighting.

below the turn-on voltage. However, above the turn-on voltage, the current flow through the diode path may become more dominant than that via the leakage path, which may result in increased efficiency.

Furthermore, a paper-based OLED lighting was demonstrated using the electrodes fabricated via the hot pressing method with the DFR insulator. A schematic illustration of the paper-based OLED lighting is shown in Fig. 4(a). The first step of the fabrication of paper-based OLED lighting was the preparation of paper-based patterned bottom electrodes with a planarization layer. As the paper substrate is opaque, the OLED lighting with the paper-based bottom electrode should be top-emission type. The ultra-thin Al and Ag layers can be transparent; thus, Al and Ag layers with ~20-nm thicknesses were used as the top electrodes in the paper-based OLED lighting. However, owing to the high roughness of the paper substrates, the formation of continuous Al and Ag interconnects to be connected to the negative bias of the power source was difficult; thus, a planarization layer was required to use the ultra-thin top electrodes for the paper-based OLED lighting. The solid-film-type DFR had a uniform thickness and could be easily deposited on the paper substrate by hot pressing, which renders the DFR an excellent candidate for the planarization layer of the paper-based OLED lighting. The fabrication process of the paper-based bottom electrodes with DFR was similar to that of the PMMA/PET-based electrodes, where the pre-patterned DFR was placed on the electrodes on paper substrates and then hot-pressed at 150 °C under 40 MPa (Fig. 4(b)). Furthermore, the fabrication process was simple, and the DFR successfully functioned as the planarization layer for the deposition of top electrodes, and as an insulator for the preparation of the patterned bottom electrodes. The paper-based top-emitting blue OLED was successfully operated, as shown in Fig. 5(a). The turn-on voltage was 3.5 V and the maximum luminance was 157 cd/m$^2$ at 7.5 V. Without any encapsulation to protect the organic layer, the performance of the paper-based OLED lighting was difficult to measure using the typical characterization equipment operated in ambient air; thus, only the luminance could be measured in a $N_2$-filled glove box using a portable spectroradiometer.

## 4. Conclusions

In this study, we reported the simple fabrication of AgNW electrodes with desirable designs using a solid-type DFR insulator for flexible OLED lighting in a single hot-pressing step. Pre-patterned DFR films were attached onto the AgNW electrodes by hot pressing. The DFR films acted as an insulating layer, thereby forming desirable designs of AgNW electrodes. In addition, the AgNWs were embedded into PMMA during the single hot-pressing step, which sufficiently reduced the RMS roughness of the AgNW electrodes to ~4.1 nm for application in OLED lighting. The patterned and embedded AgNW electrodes with a DFR were successfully applied to the bottom electrodes of OLED lighting, which exhibited a turn-on voltage of 2.8 V and maximum luminance of 27,341 cd/m$^2$ at 6.5 V. The AgNW-based OLED performance was similar to the performance of the ITO-based OLED, whose turn-on voltage and maximum luminance were 3.0 V and 22,554 cd/m$^2$ at 6.8 V, respectively. Furthermore, a paper-based OLED lighting with DFR insulator was demonstrated, which functioned well in a $N_2$-filled glove box. This simple fabrication process design utilizing a DFR can be easily adopted in the industry, especially for roll-to-roll production, which will accelerate the commercialization of AgNW-based flexible OLED lightings.

Supplementary data to this article can be found online at https://doi.org/10.1016/j.matdes.2018.09.051.

## Authors' contribution

Sunho Kim and Byungil Hwang designed and conducted the experiments and wrote the paper.

## Declarations of interest

None.

## Acknowledgement

This work was supported by the National Research Foundation (NRF) of Korea, which is funded by the Ministry of Science, Information and Communications Technology (Grant No. NRF- 2018R1C1B5043900).

## References

[1] V. Sharma, H. Sharma, R. Vyas, K. Sachdev, Polymer-metal-polymer (PMP) multilayer transparent electrode for organic optoelectronics, Mater. Des. 156 (2018) 135–142.
[2] K.-H. Ok, J. Kim, S.-R. Park, Y. Kim, C.-J. Lee, S.-J. Hong, M.-G. Kwak, N. Kim, C.J. Han, J.-W. Kim, Ultra-thin and smooth transparent electrode for flexible and leakage-free organic light-emitting diodes, Sci. Rep. 5 (2015).
[3] S. Hwan Ko, A dual-scale metal nanowire network transparent conductor for highly efficient and flexible organic light emitting diodes, Nanoscale 9 (2017) 1978–1985.
[4] S. Yin, W. Zhu, Y. Deng, Y. Peng, S. Shen, Y. Tu, Enhanced electrical conductivity and reliability for flexible copper thin-film electrode by introducing aluminum buffer layer, Mater. Des. 116 (2017) 524–530.
[5] M. Bauch, T. Dimopoulos, Design of ultrathin metal-based transparent electrodes including the impact of interface roughness, Mater. Des. 104 (2016) 37–42.
[6] C.-H. An, S. Kim, H.-J. Lee, B. Hwang, Facile patterning using dry film photo-resists for flexible electronics: Ag nanowire networks and carbon nanotube networks, J. Mater. Chem. C 5 (2017) 4804–4809.
[7] Y. Fang, Z. Wu, J. Li, F. Jiang, K. Zhang, Y. Zhang, Y. Zhou, J. Zhou, B. Hu, High-performance hazy silver nanowire transparent electrodes through diameter tailoring for semitransparent photovoltaics, Adv. Funct. Mater. 28 (2018) 1705409.
[8] K.A. Sierros, N.J. Morris, K. Ramji, D.R. Cairns, Stress–corrosion cracking of indium tin oxide coated polyethylene terephthalate for flexible optoelectronic devices, Thin Solid Films 517 (2009) 2590–2595.
[9] T. Gao, B. Wang, B. Ding, J.-k. Lee, P.W. Leu, Uniform and ordered copper nanomeshes by microsphere lithography for transparent electrodes, Nano Lett. 14 (2014) 2105–2110.
[10] H. Wu, D. Kong, Z. Ruan, P.-C. Hsu, S. Wang, Z. Yu, T.J. Carney, L. Hu, S. Fan, Y. Cui, A transparent electrode based on a metal nanotrough network, Nat. Nanotechnol. 8 (2013) 421.
[11] S.-H. Jo, Y.-K. Lee, J.-W. Yang, W.-G. Jung, J.-Y. Kim, Carbon nanotube-based flexible transparent electrode films hybridized with self-assembling PEDOT, Synth. Met. 162 (13–14) (2012) 1279–1284.

[12] T.M. Barnes, J.D. Bergeson, R.C. Tenent, B.A. Larsen, G. Teeter, K.M. Jones, J.L. Blackburn, J. van de Lagemaat, Carbon nanotube network electrodes enabling efficient organic solar cells without a hole transport layer, Appl. Phys. Lett. 96 (2010) 118.
[13] K.C. Kwon, S. Kim, C. Kim, J.-L. Lee, S.Y. Kim, Fluoropolymer-assisted graphene electrode for organic light-emitting diodes, Org. Electron. 15 (2014) 3154–3161.
[14] G. Yang, C. Lee, J. Kim, F. Ren, S.J. Pearton, Flexible graphene-based chemical sensors on paper substrates, Phys. Chem. Chem. Phys. 15 (2013) 1798–1801.
[15] B. Hwang, C.-H. An, S. Becker, Highly robust ag nanowire flexible transparent electrode with UV-curable polyurethane-based overcoating layer, Mater. Des. 129 (2017) 180–185.
[16] A.G. Ricciardulli, S. Yang, G.J.A. Wetzelaer, X. Feng, P.W. Blom, Hybrid silver nanowire and graphene-based solution-processed transparent electrode for organic optoelectronics, Adv. Funct. Mater. 28 (2018) 1706010.
[17] M. Arefpour, M. Almasi Kashi, F. Khansari Barzoki, M. Noormohammadi, A. Ramazani, Electrodeposited metal nanowires as transparent conductive electrodes: their release conditions, electrical conductivity, optical transparency and chemical stability, Mater. Des. 157 (2018) 326–336.
[18] H. Kim, G. Lee, S. Becker, J.-S. Kim, H. Kim, B. Hwang, Novel patterning of flexible and transparent ag nanowire electrodes using oxygen plasma treatment, J. Mater. Chem. C 6 (2018) 9394–9398.
[19] J.-J. Chen, S.-L. Liu, H.-B. Wu, E. Sowade, R.R. Baumann, Y. Wang, F.-Q. Gu, C.-R.-L. Liu, Z.-S. Feng, Structural regulation of silver nanowires and their application in flexible electronic thin films, Mater. Des. 154 (2018) 266–274.
[20] H. Yoon, D.S. Shin, B. Babu, T.G. Kim, K.M. Song, J. Park, Control of copper nanowire network properties and application to transparent conducting layer in led, Mater. Des. 132 (2017) 66–71.
[21] J.-Y. Lee, S.T. Connor, Y. Cui, P. Peumans, Solution-processed metal nanowire mesh transparent electrodes, Nano Lett. 8 (2008) 689–692.
[22] C. Lee, H. Kim, B. Hwang, Fracture behavior of metal oxide/silver nanowire composite electrodes under cyclic bending, J. Alloys Compd. 773 (2019) 361–366.
[23] Y. Jin, D. Deng, Y. Cheng, L. Kong, F. Xiao, Annealing-free and strongly adhesive silver nanowire networks with long-term reliability by introduction of a nonconductive and biocompatible polymer binder, Nanoscale 6 (2014) 4812–4818.
[24] J. Lee, I. Lee, T.S. Kim, J.Y. Lee, Efficient welding of silver nanowire networks without post-processing, Small 9 (2013) 2887–2894.
[25] J. Ahn, J.-W. Seo, J.Y. Kim, J. Lee, C. Cho, J. Kang, S.-Y. Choi, J.-Y. Lee, Self-supplied nano-fusing and transferring metal nanostructures via surface oxide reduction, ACS Appl. Mater. Interfaces 8 (2016) 1112–1119.
[26] X. Li, H. Park, M.H. Lee, B. Hwang, S.H. Kim, S. Lim, High resolution patterning of ag nanowire flexible transparent electrode via electrohydrodynamic jet printing of acrylic polymer-silicate nanoparticle composite overcoating layer, Org. Electron. 62 (2018) 400–406.
[27] Z. Yu, Q. Zhang, L. Li, Q. Chen, X. Niu, J. Liu, Q. Pei, Highly flexible silver nanowire electrodes for shape-memory polymer light-emitting diodes, Adv. Mater. 23 (2011) 664–668.
[28] L. Lian, D. Dong, D. Feng, G. He, Low roughness silver nanowire flexible transparent electrode by low temperature solution-processing for organic light emitting diodes, Org. Electron. 49 (2017) 9–18.
[29] E. Jung, C. Kim, M. Kim, H. Chae, J.H. Cho, S.M. Cho, Roll-to-roll preparation of silver-nanowire transparent electrode and its application to large-area organic light-emitting diodes, Org. Electron. 41 (2017) 190–197.
[30] S. Kim, T.G. Yun, C. Kang, M.-J. Son, J.-G. Kang, I.-H. Kim, H.-J. Lee, C.-H. An, B. Hwang, Facile fabrication of paper-based silver nanostructure electrodes for flexible printed energy storage system, Mater. Des. 151 (2018) 1–7.
[31] D.C. Choo, T.W. Kim, Degradation mechanisms of silver nanowire electrodes under ultraviolet irradiation and heat treatment, Sci. Rep. 7 (2017) 1696.
[32] B. Hwang, Y. An, H. Lee, E. Lee, S. Becker, Y.-H. Kim, H. Kim, Highly flexible and transparent ag nanowire electrode encapsulated with ultra-thin $Al_2O_3$: thermal, ambient, and mechanical stabilities, Sci. Rep. 7 (2017) 41336.
[33] A. Nakamura, T. Ohashi, K. Yamamoto, J. Ishihara, T. Aoki, J. Temmyo, H. Gotoh, Full-color electroluminescence from ZnO-based heterojunction diodes, Appl. Phys. Lett. 90 (2007) 093512.
[34] J.-Y. Lee, J.H. Lee, H.S. Kim, W.S. Han, H.K. Cho, J.Y. Moon, H.S. Lee, Effect of interface on n-ZnO/p-GaN heterojunction light-emitting diodes, J. Korean Phys. Soc. 55 (2009) 1568–1571.
[35] L. Oleg, P. Thierry, V. Bruno, Low-voltage UV-electroluminescence from ZnO-nanowire array/P-GaN light-emitting diodes, Adv. Mater. 22 (2010) 3298–3302.
[36] S. Kim, B. Kim, S.M. Cho, H.-J. Lee, B. Hwang, Etchant-free patterning of silver nanowire transparent electrode using dry-film photoresists for organic light-emitting diodes, Mater. Lett. 209 (2017) 433–436.